Palaeogeography, Palaeoclimatology, Palaeoecology 440 (2015) 496–505

Contents lists available at ScienceDirect

Palaeogeography, Palaeoclimatology, Palaeoecology

journal homepage: www.elsevier.com/locate/palaeo

Indication of millennial-scale moisture changes by the temporal distribution of Holocene calcareous root tubes in the deserts of the Alashan Plateau, Northwest China

Zhuolun Li *, Nai'ang Wang, Ruolan Li, Kai Ning, Hongyi Cheng, Liqiang Zhao

College of Earth and Environmental Sciences, Center for Climatic Change and Hydrological Cycle in Arid Region, Lanzhou University, Lanzhou 730000, China

ARTICLE INFO

Article history:
Received 10 February 2015
Received in revised form 7 September 2015
Accepted 17 September 2015
Available online 30 September 2015

Editor: Paul Hesse

Keywords:
Rhizoliths
Secondary carbonate
Paleo-effective moisture
Asian monsoon
Sand dune
Arid region

ABSTRACT

Calcareous root tubes or rhizoliths have a strong potential for paleoenvironmental studies, especially in reconstructing paleoenvironmental conditions and paleovegetation. Previous studies suggested that the effectivity of the moisture level affects the formation of calcareous root tubes in the deserts of the Alashan Plateau, Northwest China. However, it remains unclear whether the temporal distribution of calcareous root tubes can be used to reconstruct paleo-effective moisture in this area. In this study, based on conventional ^{14}C dating results of 34 Holocene calcareous root tube samples collected from the Badain Jaran Desert, the Tengger Desert and the Ulan Buh Desert in the Alashan Plateau of northwestern China, millennial-scale changes in paleo-effective moisture during the Holocene in this area were reconstructed. The frequency of the ^{14}C dating results demonstrates that ~62% of the Holocene samples were dated to 7–5 cal kyr BP, and ~38% of the Holocene samples were dated to 4–2 cal kyr BP, indicating an arid period during the early Holocene (before 8.0 cal kyr BP), a humid period during the mid-Holocene (8.0–5.0 cal kyr BP) and a humid to arid period during the late Holocene (after 5.0 cal kyr BP). The reconstruction results were consistent with other previous reconstruction results from lake sediments and aeolian sand–lacustrine sequences, which indicated that temporal distribution of calcareous root tubes can reflect millennial-scale changes in paleo-effective moisture in this area. However, a single sample could indicate local environmental changes that may differ from the overall desert environmental changes. Hence, the relatively humid environmental record obtained from the presence of calcareous root tubes is a local signal or a regional signal that should be noted.

1. Introduction

Calcareous root tubes, which are also called rhizoliths or calcified roots, are products of terricolous plants and are formed by encrustation of plant roots by secondary carbonates (Klappa, 1980; Gocke et al., 2011a). Calcareous root tubes have been frequently described and almost invariably occur in calcareous soils and underlying soil parent materials in regions with a pronounced seasonal moisture regime (Jaillard et al., 1991; Alonso-Zarza, 2003; Gocke et al., 2014a), such as southwest Slovenia (Kosir, 2004), western Mediterranean (Klappa, 1980), southwest Germany (Gocke et al., 2010, 2011a) and southern France (Jaillard et al., 1991). They form faster than other forms of secondary carbonate that are more distant from roots (Gocke et al., 2011b). Moreover, they are also preserved in loess–paleosol sequences (Barta, 2011), and their isotopic composition is used for paleoenvironmental reconstruction (Wright et al., 1995; Wang et al., 2004; Wang and Greenberg, 2007; Gocke et al., 2011a; Huguet et al., 2012; Gallant et al., 2014; Gocke et al., 2014b; Koeniger et al., 2014). In micromorphology, calcified root cells (calcifications of the root cells) usually occur in calcareous root tubes and also have specific environmental significance (Jaillard et al., 1991; Alonso-Zarza, 2003). Previous studies focused on their classification (Klappa, 1980), isotopic composition (Gocke et al., 2011a), macro- and micromorphology (Jaillard et al., 1991; Kosir, 2004; Barta, 2014) and chronological context (Gocke et al., 2011a; Li et al., 2015). These studies reveal a high potential for calcareous root tubes to be used in paleoenvironmental studies, especially in reconstructing paleoenvironmental conditions and paleovegetation (Wang and Greenberg, 2007; Barta, 2014; Gocke et al., 2014b). Therefore, investigating calcareous root tubes for paleoenvironmental conditions aids in the evaluation of the reliability of using these materials to assess past global changes.

In arid regions of northwestern China, calcareous root tubes are distributed across the deserts of the Alashan Plateau (Li et al., 2015), most of which were dated to Marine Isotope Stage (MIS) 3 and the Holocene (Gao et al., 1993; Yang, 2000; Chen et al., 2004; Li et al., 2015). Moreover, Li et al. (2015) suggested that the moisture level affects the formation of calcareous root tubes, and the presence of calcareous root tubes indicates the occurrence of periods with relatively humid conditions in the deserts of the Alashan Plateau. However, it is

* Corresponding author. Tel.: +86 13619369339.
E-mail address: lizhuolunlzl@163.com (Z. Li).

http://dx.doi.org/10.1016/j.palaeo.2015.09.023
0031-0182/

still unclear whether the temporal distribution of calcareous root tubes can be used effectively to reconstruct paleo-effective moisture in this area.

For this study, we present the ^{14}C dating results of 34 Holocene calcareous root tube samples collected from the Badain Jaran Desert, the Tengger Desert and the Ulan Buh Desert in the Alashan Plateau of northwestern China (Fig. 1) and subsequently use the temporal distribution of the samples to reconstruct Holocene effective moisture variations.

2. Study area

The Alashan Plateau is located in an arid region of northwestern China with an area of approximately 300,000 km^2 (Fig. 1). The Plateau has an altitude of 1500–2000 m above sea level (a.s.l.). The area is outside the direct influence of the Asian summer monsoon and Westerlies, and the present-day climate is extremely dry and continental. The plateau comprises the Badain Jaran Desert, the Tengger Desert, the Ulan Buh Desert and other deserts (Wang et al., 2011).

The Badain Jaran Desert lies in the western portion of the Alashan Plateau (Fig. 1). With an area of approximately 52,100 km^2, it is the second-largest desert in China (Zhu et al., 2010). The mean winter and summer temperatures in this area are −9 and 25 °C, respectively. The desert is characterized by a strongly continental climate with a mean annual precipitation of 90–115 mm in the south and 35–43 mm in the north (Ma et al., 2011). The annual precipitation is ~100 mm in the hinterland of the Badain Jaran Desert (Z. Li et al., 2013; Ma et al., 2014), whereas the mean annual evaporation rate from water surfaces is ~1000 mm/year (Yang et al., 2010, 2011). To the north of the desert, the mean annual evaporation is 2345 mm (Z. Li et al., 2013). Moreover, the conventional precipitation (below 5 mm), accounting for approximately 90% of all rain events in the desert, evaporates from the mega-dune surface in 1–3 days (Ma et al., 2014).

The Tengger Desert (Fig. 1), with an area of approximately 42,700 km^2, is the fourth-largest desert in China (Zhu et al., 1980). It is located in the southeastern portion of the Alashan Plateau (Fig. 1). The Tengger Desert is primarily covered with mobile sand dunes, and its elevation ranges from 1000 to 1500 m a.s.l. The mean annual temperature is 8 °C, and the regional mean annual precipitation ranges from 125 to 160 mm, whereas the mean annual potential evaporation is approximately 2600 mm.

The Ulan Buh Desert, with an area of 11,000 km^2 (Wang, 2003), lies in the eastern portion of the Alashan Plateau (Fig. 1). The desert is primarily covered with mobile sand dunes, its elevation ranges from 1028 to 1054 m, and it is on the boundary between arid and semi-arid China (Yang et al., 2011). At present, the mean annual temperature in the area is 7 °C and the mean annual precipitation is 103 mm, with 65% of the mean annual precipitation occurring during the summer; the regional mean annual potential evaporation is 2957 mm. The area has typical desert vegetation including *Haloxylon ammodendron*, *Caragana Korshinskii*, *Artemisia desterorum*, *Ammopiptanthus mongolicus* and *Achnatherun splendes* (Wu, 2007).

3. Material and methods

3.1. Morphological characters and samples collected

In this study, gray–white calcareous root tubes from 45 localities in the deserts of the Alashan Plateau were collected (Fig. 2). All the localities contained sandy soils with a median grain size of 0.2–0.4 mm, and a

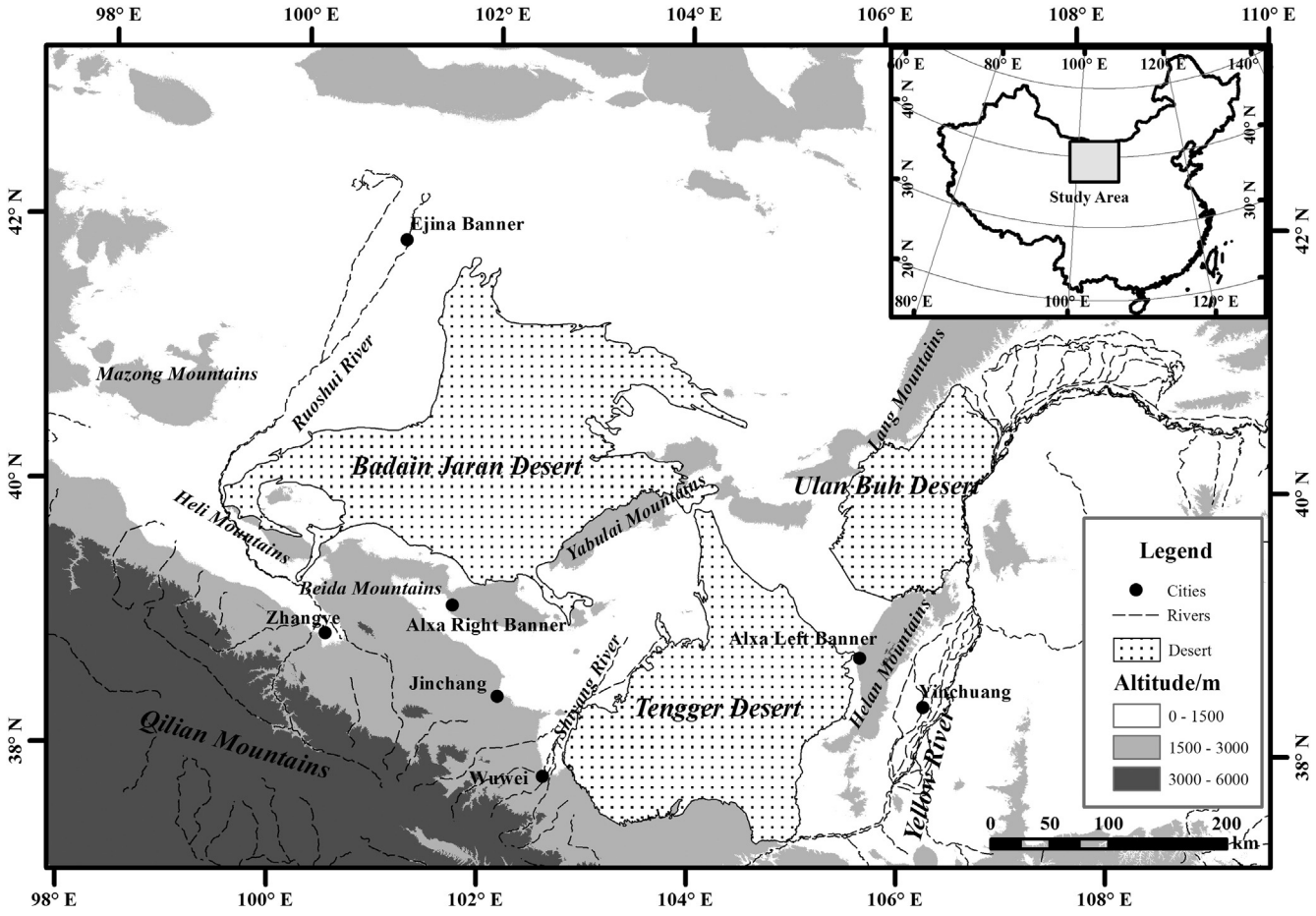

Fig. 1. Location of the study area.

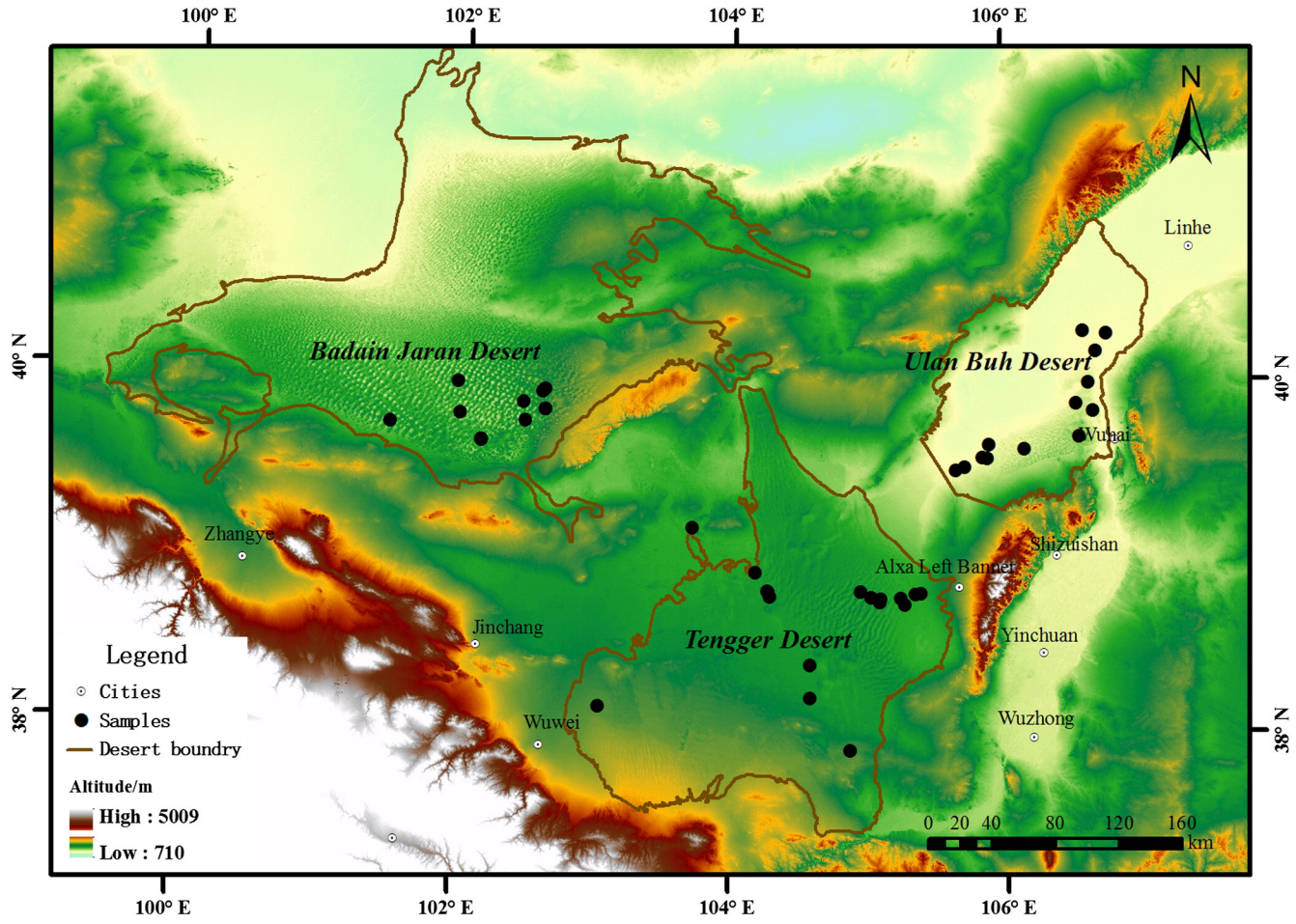

Fig. 2. Locations of the calcareous root tubes sampled from the deserts of the Alashan Plateau.

sand layer of more than 1 m deep. Calcareous root tubes were distributed at the localities from the surface layer to a depth of 18 cm (Fig. 3). In the Badain Jaran Desert, the calcareous root tubes were located on the surface of megadunes at different altitudes; most of the calcareous root tubes were horizontal (Fig. 3a and b). In the Tengger Desert and the Ulan Buh Desert, the calcareous root tubes were located on the surface of the inter-dune bottomland and were oriented both horizontally and vertically (Fig. 3c, d and e). Lengths of the horizontal calcareous root tubes vary from a few centimeters to tens of centimeters (Fig. 3a and b); the longest recorded in this study was 57 cm long and was located in the Badain Jaran Desert (Fig. 3b). Lengths of the vertical calcareous root tubes were between 10 and 30 cm in this study (Fig. 3c, d and e), most of which were down to less than 10 cm in the sand (Fig. 3c). The longest vertical tube in the Tengger Desert, with a length of 28 cm, was down to 18 cm below the surface in the sand layer (Fig. 3d and e).

Based on scanning electron microscope (SEM) images (Fig. 4) the outermost and most indurated ring of calcareous root tubes is composed of aeolian sands with incipient carbonate cements, probably of calcite. Other minerals like quartz, feldspars, and micas, which are attributed to primary aeolian sands, occur only close to the outer boundary areas (Fig. 4a and b). Moreover, calcified fungal hyphae mycelia and aggregates of crystals were shown by SEM images (Fig. 4c and d).

All samples were collected from the surface of the sand layers. Fifteen samples were collected from the Badain Jaran Desert, seventeen samples were collected from the Tengger Desert, and thirteen samples were collected from the Ulan Buh Desert. Thus, a total of 45 samples were collected (Fig. 2); among them, 31 samples were presented by Li et al. (2015).

3.2. Laboratory methods

Samples were dated by conventional radiocarbon analyses. The conventional ^{14}C ages were measured at the Laboratory of Chronology, Lanzhou University, China. Radiocarbon ages were converted to calendar year ages using the Intcal 13 model of the Calib 7.0 program (Reimer et al., 2013), accounting for temporal variations in the ^{14}C activity of the atmosphere.

3.3. Calculations and statistics

The results of ^{14}C dating of secondary carbonate could be affected by various factors. For example, Gocke et al. (2011a) suggested that a feature of recrystallization that occurred in calcareous root tubes could not be significantly younger than the surrounding micritic carbonate in the loess–paleosol sequence at Nussloch, SW Germany. This has contributed to the lower reliability of ^{14}C dates for calcareous root tubes at the century scale (Gocke et al., 2011b). Even without the recrystallization effect, it is still difficult to improve the reliability of the dating results at the century scale because of the presence of other confounding factors such as the incorporation of older and younger C. However, the majority of carbonate materials in the calcareous root tubes were not recrystallized after segregation, justifying their suitability for radiocarbon dating in loess–paleosol sequence at Nussloch, SW Germany (Gocke et al., 2011a). Moreover, Li et al. (2015) found that calcareous root tubes in the deserts of the Alashan Plateau could be used as ^{14}C dating material and that the ^{14}C dates for calcareous root tubes were

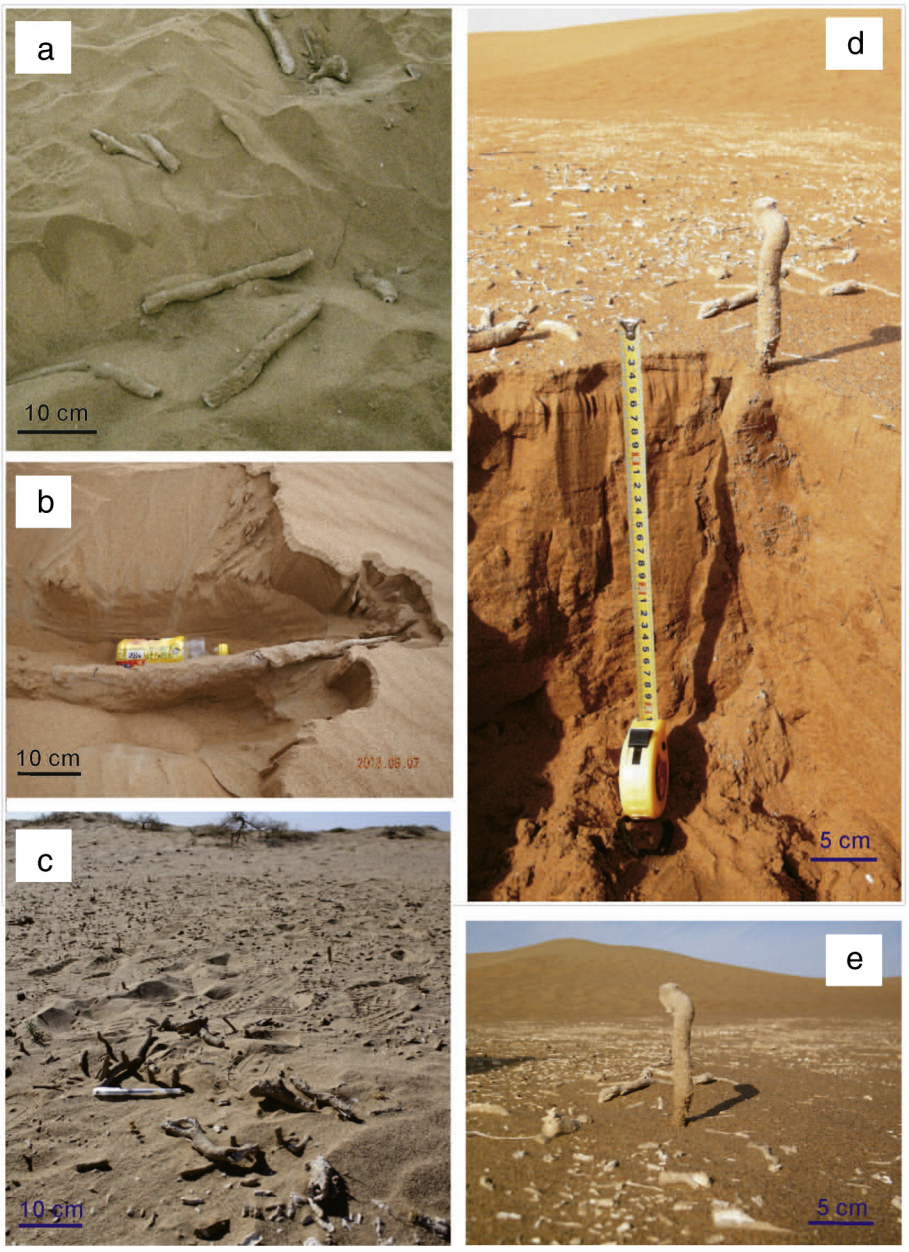

Fig. 3. (a) Calcareous root tubes were horizontally located on the surface of megadunes in the Badain Jaran Desert with lengths of a few centimeters. (b) Horizontal calcareous root tubes occurred in the Badain Jaran Desert with a length of 57 cm. (c) Vertical and horizontal calcareous root tubes occurred in the Ulan Buh Desert with a length of 10 cm. (d) and (e) The longest vertical calcareous root tubes in the Tengger Desert had a length of 28 cm and were down to 18 cm depth in the sand layer.

reliable within the millennial scale for Holocene ages. This was consistent with the results previously reported by Kuzyakov et al. (2006), Pustovoytov et al. (2007) and Gocke et al. (2011b). Based on the above findings, the numbers of ^{14}C ages in each millennium were counted in this study, as a possible recrystallization in calcareous root tubes would not affect the reliability of ^{14}C dating results at the millennial scale for Holocene ages. Then, the frequency of ^{14}C dates in each millennium from the entire area, the Badain Jaran Desert, the Tengger Desert and the Ulan Buh Desert, was calculated respectively.

3.4. Proxy interpretation

The effectivity of the moisture level and soil conditions probably affect the formation of calcareous root tubes (Jones and Ng, 1988; Wright, 1994). The formation of calcareous root tubes requires net moisture deficits; however, net moisture surpluses or deficits both impact calcareous root tube formation. Cerling (1984) considered that secondary (pedogenic) carbonates form when the mean annual precipitation is lower than 750 mm. Moreover, Birkland (1999) suggested that the highest accumulations of secondary carbonate occur under semiarid conditions with mean annual precipitation less than approximately 500 mm. Therefore, environments that are too humid or too arid may not be suitable for the formation of calcareous root tubes.

In desert areas of the Alashan Plateau, which are typically arid regions with low precipitation (100 mm/yr) and high evaporation (more than 1 000 mm/yr), net moisture deficits are greater than those in semi-arid and semi-humid regions. Rain and heat over the same period is a typical climatic characteristic in this area, with the highest amount of evaporation and precipitation occurring simultaneously in summer (Z. Li et al., 2013; Ma et al., 2014). Evaporation is consistently higher than precipitation across all seasons, leading to a net moisture deficit in the entire year (Z. Li et al., 2013; Ma et al., 2014). Moreover,

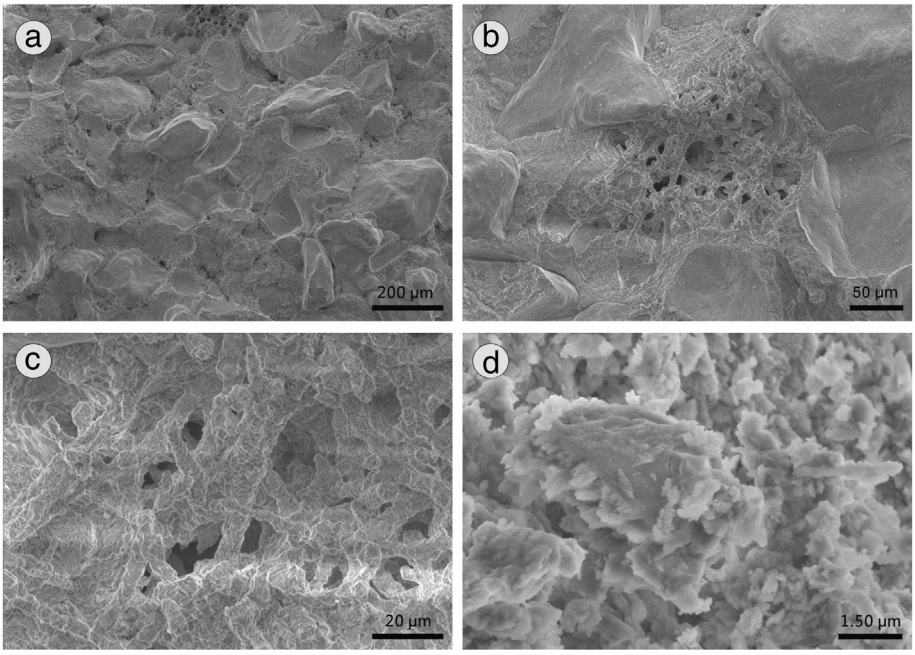

Fig. 4. Scanning electron microscope (SEM) images. (a) SEM image of the outermost and most indurated ring of calcareous root tubes. It is composed of aeolian sands with incipient carbonate cements, probably of calcite. (b) Detailed view of (a). (c) SEM image of calcified fungal hyphae mycelia on exterior surfaces. (d) SEM image of aggregates of crystals, probably of calcite.

all the precipitation in a typical rain event (below 5 mm) could evaporate from the mega-dune surface in 1–3 days (Ma et al., 2014). In that case, it is difficult for the ground surface to stay moist when the amount of precipitation is decreasing, leading to unfavorable soil conditions for calcareous root tube formation in this area (Li et al., 2015). Furthermore, whether extreme precipitation followed by strongly enhanced evaporation could impact calcareous root tube formation in this area is still unclear. In the hinterland of the Badain Jaran Desert, a continuation of the strong evaporation process usually occurs after extreme precipitation (Ma et al., 2014), which in theory will lead to calcite precipitation. However, previous researches (Gao et al., 1993; Yang, 2000; Chen et al., 2004; Li et al., 2015) have reported more than 50 calcareous root tube ages, and the dating results suggested that no modern calcareous root tubes occurred in this area. These findings suggest that extreme precipitation followed by strongly enhanced evaporation may not support active formation of calcareous root tubes in this area.

Meanwhile, calcareous root tubes could form during periods of relatively high humidity in these study areas, thus indicating a relatively humid environment (Li et al., 2015). During the relatively humid periods (e.g. 7–5 cal kyr BP), strong summer monsoons led to a relatively large increase in moisture availability (Yang et al., 2011), though we speculated that net moisture deficits still occurred in the entire year. Furthermore, paleoclimate reconstructed results by multi-proxy (grain size, carbonate, TOC, C/N and $\delta^{13}C$ of organic matter from lake sediments) have indicated that, on the millennial scale, the mean annual precipitation could not increase to 500 mm in these areas during the Holocene (Yang, 2000; Zhang et al., 2004; Li et al., 2009; Yang et al., 2011). Therefore, large numbers of calcareous root tubes in this area reflect a relatively humid environment; arid environments were not suited for calcareous root tube formation, and the number of calcareous root tubes should decrease. Thus, changes in the frequency of the ^{14}C dates in each millennium could indicate the effective moisture changes in the overall desert.

We interpreted frequencies of the calcareous root tubes ^{14}C dating results on the millennial scale as a proxy of effective moisture. High frequency indicates a humid environment, which is suitable for the formation of calcareous root tubes, whereas low frequency indicates an arid environment.

4. Results

4.1. ^{14}C dating results

Li et al. (2015) presented 31 calcareous root tubes ages, and 20 calcareous root tube samples were dated to the Holocene (Table 1). In this study, 14 calcareous root tube samples from the Ulan Buh Desert and the Badain Jaran Desert were dated to the Holocene (Table 1). Hence, 34 Holocene calcareous root tube ages (Table 1) were used to calculate the frequency of the ^{14}C dates in each millennium.

The frequency of the ^{14}C dating results reveal that ~62% of the Holocene samples were dated to 7–5 cal kyr BP and ~38% of the Holocene samples were dated to 4–2 cal kyr BP (Fig. 5a). In the Badain Jaran Desert, all Holocene samples were dated to 7–5 cal kyr BP (Fig. 5b); 65% and 42% of the Holocene samples were dated to those periods from the Tengger Desert and the Ulan Buh Desert, respectively (Fig. 5c and d). Moreover, frequencies of ^{14}C dating results are 35.3% in the Tengger Desert and 54% in the Ulan Buh Desert during 4–0 cal kyr BP. The results reveal that frequencies of ^{14}C ages in the mid-Holocene (7–5 cal kyr BP) decreased from the western part to the eastern part in the deserts of the Alashan Plateau.

4.2. Effective moisture reconstructions

According to the frequency of the ^{14}C dating results (Fig. 5), Holocene millennial-scale effective moisture changes in the deserts of the Alashan Plateau can be divided into three stages:

Stage 1 (before 8.0 cal kyr BP): arid period. In this study, the capacity of the sample size (45) meets the basic requirements of the statistics, and the samples were widely collected from the deserts of the Alashan Plateau (Fig. 2). However, no sample was dated from this stage, which indicated that the overall desert effective moisture is not suited for prolific calcareous root tubes formation. Therefore, the climate was arid in this period from the proxy interpretation of the frequency of the ^{14}C dating results.

Stage 2 (8.0–5.0 cal kyr BP): humid period. A high frequency of ^{14}C dating results occurred during this time period, indicating a humid environment in the deserts of Alashan Plateau. Moreover, the highest

Table 1
^{14}C ages of Holocene samples collected from the deserts of the Alashan Plateau.

Lab. no.	Latitude/N	longitude/E	^{14}C yr BP	cal yr BP (2σ)	Location	References
LUG12-183	38°09′13.5″	103° 31′ 5.0″	5731 ± 66	6513 (6351–6675)	The Tengger Desert	Li et al. (2015)
LUG11-129	38°47′2.1″	105°01′15.3″	5220 ± 58	6039 (5895–6183)	The Tengger Desert	Li et al. (2015)
LUG11-174	38°48′21.2″	105°22′59.9″	6382 ± 59	7301 (7177–7425)	The Tengger Desert	Li et al. (2015)
LUG11-175	38°48′9.5″	105°20′30.6″	5198 ± 57	5969 (5760–6178)	The Tengger Desert	Li et al. (2015)
LUG11-176	38°46′42.1″	105°14′28.9″	2262 ± 72	2259 (2061–2457)	The Tengger Desert	Li et al. (2015)
LUG11-178	38°46′33.7″	105°05′35.6″	5118 ± 59	5859 (5727–5990)	The Tengger Desert	Li et al. (2015)
LUG11-179	38°48′58.9″	104°56′43.3″	4839 ± 58	5523 (5333–5712)	The Tengger Desert	Li et al. (2015)
LUG11-180	38°45′22.2″	105°05′13.1″	3339 ± 49	3573 (3455–3691)	The Tengger Desert	Li et al. (2015)
LUG11-181	38°44′30.4″	105°16′7.4″	2970 ± 51	3150 (2971–3328)	The Tengger Desert	Li et al. (2015)
LUG11-187	39°10′37.1″	103°42′59.1″	4630 ± 55	5324 (5068–5579)	The Tengger Desert	Li et al. (2015)
LUG11-188	38°55′31.8″	104°10′34.7″	4891 ± 55	5612 (5482–5742)	The Tengger Desert	Li et al. (2015)
LUG11-189	38°49′16.1″	104°15′58.3″	4259 ± 54	4795 (4623–4966)	The Tengger Desert	Li et al. (2015)
LUG11-190	38°48′53.5″	104°16′24.5″	5412 ± 61	6154 (6004–6305)	The Tengger Desert	Li et al. (2015)
LUG11-191	38°47′14.5″	104°17′8.9″	3779 ± 59	4192 (3980–4404)	The Tengger Desert	Li et al. (2015)
LUG11-192	38°24′1.7″	104°34′50.3″	4765 ± 54	5462 (5326–5597)	The Tengger Desert	Li et al. (2015)
LUG11-193	38°12′48.4″	104°34′50.3″	5989 ± 66	6829 (6670–6988)	The Tengger Desert	Li et al. (2015)
LUG11-194	37°54′59.9″	104°52′13.0″	4090 ± 60	4630 (4438–4821)	The Tengger Desert	Li et al. (2015)
LUG11-186	39°56′56.6″	102°37′23.4″	6843 ± 65	7701 (7578–7824)	The Badain Jaran Desert	Li et al. (2015)
LUG11-195	39°56′13.9″	102°36′20.1″	5564 ± 66	6353 (6218–6488)	The Badain Jaran Desert	Li et al. (2015)
BA110772	39°46′7.9″	102°28′34.8″	4585 ± 35	5256 (5062–5449)	The Badain Jaran Desert	Li et al. (2015)
LUG13-56	39°57′00″	102°37′40.2″	6584 ± 64	7452 (7335–7568)	The Badain Jaran Desert	This study
LUG13-57	39°30′31.1″	105°38′40.4″	5731 ± 60	6534 (6404–6604)	The Ulan Buh Desert	This study
LUG13-58	39°31′21.7″	105°42′34.2″	6791 ± 71	7650 (7513–7786)	The Ulan Buh Desert	This study
LUG13-59	39°34′40.4″	105°50′30.6″	4254 ± 55	4791 (4617–4964)	The Ulan Buh Desert	This study
LUG13-60	39°34′28.7″	105°52′23.3″	3328 ± 52	3570 (3448–3692)	The Ulan Buh Desert	This study
LUG13-61	39°37′40.3″	106°08′54.8″	3272 ± 52	3498 (3385–3611)	The Ulan Buh Desert	This study
LUG13-62	39°41′36.5″	106°33′7.1″	3755 ± 55	4137 (3929–4345)	The Ulan Buh Desert	This study
LUG13-63	39°50′18.5″	106°39′14.1″	3566 ± 53	3879 (3698–4060)	The Ulan Buh Desert	This study
LUG13-64	39°52′51.6″	106°32′6.3″	4062 ± 56	4617 (4420–4813)	The Ulan Buh Desert	This study
LUG13-65	40°16′45.3″	106°45′44.6″	6125 ± 61	6986 (6801–7171)	The Ulan Buh Desert	This study
LUG13-66	40°17′29.7″	106°35′25.7″	4094 ± 56	4631(4440–4821)	The Ulan Buh Desert	This study
LUG13-67	40°10′41.2″	106°40′58.4″	5649 ± 60	6451 (6301–6601)	The Ulan Buh Desert	This study
LUG13-69	39°59′59.8″	106°37′34.5″	6198 ± 64	7102 (6946–7257)	The Ulan Buh Desert	This study
LUG13-70	39°39′1.8″	105°53′17.9″	5573 ± 61	6382 (6280–6483)	The Ulan Buh Desert	This study

frequency of ^{14}C dating results occurred at 7 cal kyr BP in the Badain Jaran Desert, and the frequency of ^{14}C dating results decreased between 6 and 5 cal kyr BP. This suggests that the effective moisture decreased from 7 to 5 cal kyr BP. In the Tengger Desert, the highest frequency of ^{14}C dating results occurred at 5 cal kyr BP, which indicates that the effective moisture increased during this period. In the Ulan Buh Desert, the highest frequency of ^{14}C dating results occurred at 6 cal kyr BP, indicating effective moisture increasing from 7 to 6 cal kyr BP.

Stage 3 (after 5.0 cal kyr BP): humid to arid period. No sample from the Badain Jaran Desert was dated from this stage. Furthermore, the frequency of ^{14}C dating results decreased during this period, indicating that the effective moisture decreased in the Tengger Desert. The frequency of ^{14}C dating results was highest at 4 cal kyr BP in the Ulan Buh Desert and then decreased after that period, indicating that the effective moisture decreased after 4 cal kyr BP in the Ulan Buh Desert.

5. Discussion

5.1. Comparison with previous studies

To clarify whether the frequency of ^{14}C dating results could indicate changes in effective moisture in the deserts of the Alashan Plateau and whether effective moisture records obtained from the frequency of ^{14}C dating results were consistent with other previous reconstruction results, we compared our results to other previous reconstruction results from the deserts of the Alashan Plateau (Fig. 6).

In the Badain Jaran Desert, Yang et al. (2011) compiled previously published paleoclimate records including assessments of nine lakes in the Badain Jaran Desert and established the framework of the Holocene climate history in the region. Reconstructed paleoclimate results by inter-dune lake shorelines within the Badain Jaran Desert suggested that the area was generally dry before 10 cal kyr BP, becoming wetter from 10 (particularly after 8 cal kyr BP) to 4 cal kyr BP and dry again afterward (Yang et al., 2011). The age of the highest lake stands from the four lakes studied bracket the interval between 4000 and 7500 cal yr BP, and they concluded that the climate reached maximum wetness during the middle Holocene (Yang et al., 2010). Therefore, the frequency of ^{14}C dating results in the Badain Jaran Desert is indicative of effective moisture changes, and the effective moisture record in this study is consistent with that of Yang et al. (2010, 2011) (Fig. 6).

In the Tengger Desert, based on multi-proxy (grain size, carbonate, TOC, C/N and δ^{13}C of organic matter from lake sediments) and lake-level variations, Long et al. (2010) suggested that the climate was dry in the early Holocene (9.5–7.0 cal kyr BP), humid in the mid-Holocene (7.0–4.8 cal kyr BP) and increasingly drier in the late Holocene (since 4.8 cal kyr BP) (Fig. 6). Moreover, in Zhuye Lake, located in the Tengger Desert, high lake levels existed in the mid-Holocene, indicating that the wettest stage of the Holocene occurred in this period (Zhang et al., 2004; Wang et al., 2011; Long et al., 2012). Hence, the highest frequency of ^{14}C dating results in the Tengger Desert indicates the highest effective moisture (Fig. 6).

In the Ulan Buh Desert, reconstructed paleoclimate results from a series of aeolian sand–lacustrine sequences indicated that aeolian activity prevailed before ~8.3 ka (Zhao et al., 2012), signifying that an aeolian desert environment prevailed during the early Holocene at low elevations. Then, a unified Ulan Buh paleolake containing the modern Jilantai Salt Lake covered the northern desert during 7.8–7.1 ka. The paleolake receded and broke apart after 6.5 ka (Zhao et al., 2012). Moreover, based on multi-proxy (e.g., grain size and pollen), Chen et al. (2014) suggested that the wetlands, ponds and shallow lakes formed in the northern Ulan Buh Desert only during 8–7 ka; a desert aeolian environment occupied the entire modern Ulan Buh Desert area until the middle Holocene (7–6 ka) (Chen et al., 2014). Previous studies (Zhao et al., 2012; Chen et al., 2014) have suggested that the landscape evolution of the Ulan Buh Desert indicates an arid environment before ~8.3 ka, a humid environment during 7.8–7.1 ka and an arid environment

a-
ft-
er

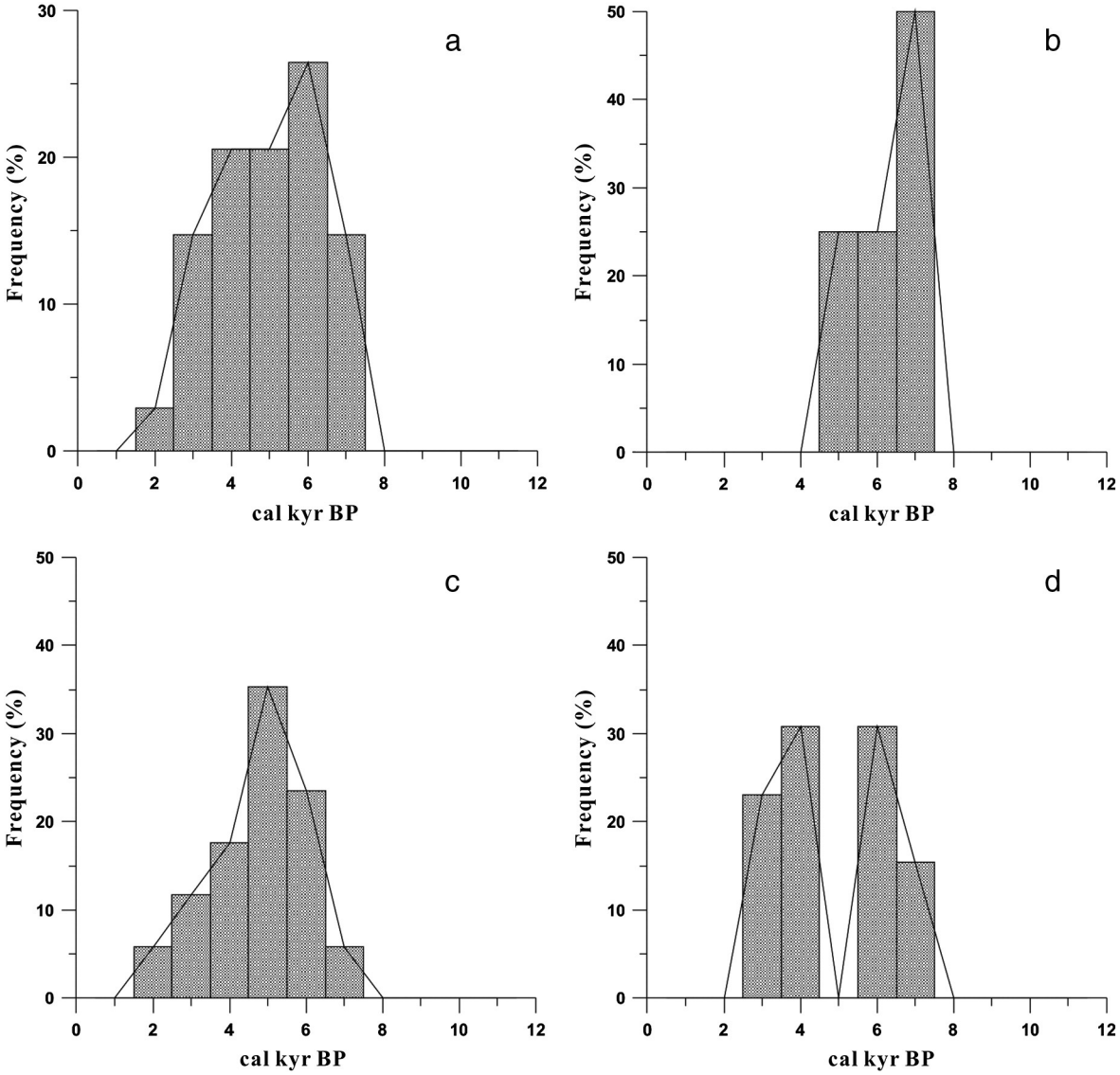

Fig. 5. Statistics for calcareous root tubes ^{14}C dating results on the millennial scale; the black line is the frequency of ^{14}C dating results. (a) Deserts of the Alashan Plateau, (b) the Badain Jaran Desert, (c) the Tengger Desert, and (d) the Ulan Buh Desert.

7 ka (Fig. 6). In this study, no calcareous root tube samples collected from the Ulan Buh Desert were dated before 8 cal ka BP or during 5 cal ka BP. The frequency of ^{14}C dating results in the Ulan Buh Desert increased during 7–6 cal ka BP and decreased during 4–3 cal ka BP. Changes in the frequency of ^{14}C dating results indicate that an arid environment occurred before 8 cal kyr BP and at 5 cal kyr BP, a humid environment occurred at 7–6 cal kyr BP and 4–3 cal kyr BP, and an arid environment occurred after 3 cal kyr BP. This indicated that changes in effective moisture after 7 cal kyr BP were not consistent with those reported by Chen et al. (2014). The main reason for the apparent discrepancies could be that Chen et al. (2014) focused on the landscape evolution of the Ulan Buh Desert during the last 90 ka, and the studied timescales did not focus on the millennial scale; there were no dating results after 7 cal kyr BP. Moreover, landscape evolution indirectly indicates changes in the effective moisture. Therefore, although changes in effective moisture during the Holocene as derived by Chen et al. (2014) and this study are not consistent, the frequency of ^{14}C dating results in the Ulan Buh Desert could indicate effective moisture changes.

Thus, based on the comparison of our results to other previous reconstruction results in the deserts of the Alashan Plateau (Fig. 6), effective moisture records obtained from the frequency of ^{14}C dating results were consistent with other previous reconstruction results, and frequency of the ^{14}C dating results could indicate changes in effective moisture in the deserts of the Alashan Plateau.

5.2. The question of applicability

In the deserts of the Alashan Plateau, the effectivity of the moisture level and soil conditions affect the formation of calcareous root tubes, and the presence of calcareous root tubes indicates relatively humid environments (Li et al., 2015). In this study, the frequency of ^{14}C dating results could indicate millennial-scale changes in effective moisture in the deserts of the Alashan Plateau. However, a single sample could indicate a local humid environment that may differ from the overall desert environment. In this area, more than one hundred lakes are located in the Badain Jaran Desert (Li et al., 2013b; Ma et al., 2014; Wu et al., 2014; Zhang et al., 2014), and there are also many inter-dune lakes located in the Tengger Desert and the Ulan Buh Desert (Zhu et al., 1980; Lai et al., 2012). In the swale around the inter-dune lakes, the soil moisture content is higher than that in megadunes and inter-dune bottomland. In this case, calcareous root tubes could form in some areas with high soil moisture content during arid periods; thus, a small quantity of samples dated to less than 3 cal kyr BP in this study (Fig. 5) could be interpreted. Hence, the relatively humid environmental

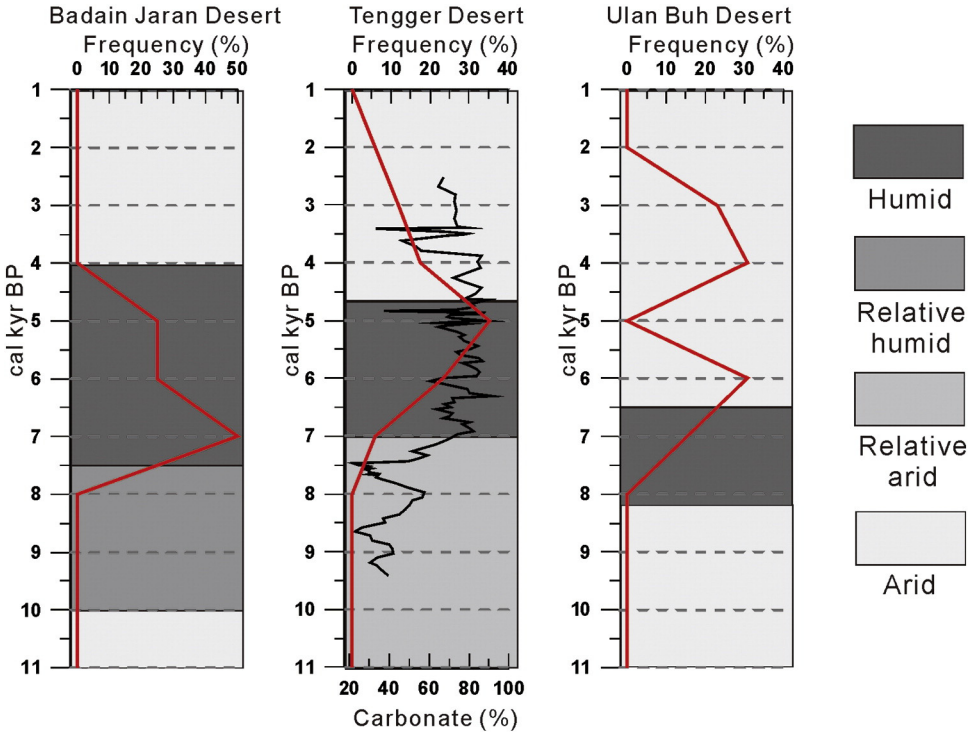

Fig. 6. Comparison of our study with other Holocene proxy records in the deserts of the Alashan Plateau. The red lines are frequencies of ^{14}C dating results in the deserts, and the shadows indicate arid or humid periods in the deserts. In the Badain Jaran Desert, shadows are based on reconstructed paleoclimate results by inter-dune lake shorelines within the Badain Jaran Desert (Yang et al., 2010, 2011). In the Tengger Desert, shadows are based on reconstructed paleoclimate results by multi-proxy (grain size, carbonate, TOC, C/N and $\delta^{13}C$ of organic matter from lake sediments) and lake-level variations (Long et al., 2010), and the black line is the carbonate (%) from lake sediments, which are taken from Long et al. (2010); In the Ulan Buh Desert, shadows are based on reconstructed paleoclimate results by a series of aeolian sand–lacustrine sequences (Zhao et al., 2012) and multi-proxy (e.g., grain size and pollen) (Chen et al., 2014). (For interpretation of the references to color in this figure legend, the reader is referred to the web version of this article.)

record obtained from the presence of calcareous root tubes is a local signal or a regional signal that should be noted.

Moreover, previous studies revealed that calcareous root tubes occurred in the layers of paleo-dunes and some lake-margin deposits, indicating different environmental significance (Yang et al., 2003; Liutkus et al., 2005). Yang (2000) dated calcareous root tubes from the paleo-dunes in the southeastern part of the Badain Jaran Desert, and the presence of calcareous root tubes in the layers of paleo-dunes indicated a relatively moister climate during the last 31,000 years (Yang et al., 2003). However, the presence of calcareous root tubes in some lake-margin deposit layers in Africa indicated an arid environment (Liutkus et al., 2005). Liutkus et al. (2005) reported that during drier periods, the paleolake receded, and water in emergent wetlands was subject to evaporation and exchange with atmospheric CO_2, resulting in calcareous root tubes (rhizolith) formation. In general, changes in soil moisture also affect the formation of calcareous root tubes and could result in calcareous root tubes having distinct environmental significance in the layers of paleo-dunes and some lake-margin deposits.

In arid regions, changes in effective moisture could be reconstructed by lake sediments (Zhang et al., 2000; Chen et al., 2008; Hartmann and Wünnemann, 2009; Li et al., 2009; Long et al., 2010; Li et al., 2013a; Wang et al., 2013) and aeolian deposition (An et al., 2000; Yang et al., 2003; Cai et al., 2012). The reliability of reconstruction results depends on the location of the section, deposition rate, chronology and interpretations of the proxy records (Chen et al., 2004; Mayewski et al., 2004; Feng et al., 2006; Zhang et al., 2006; Li et al., 2011, 2012; Wang et al., 2013). However, suitable profiles are scarce in deserts, and other factors also impact the reliability of reconstruction results (Zhang et al., 2006). Therefore, reconstruction of effective moisture changes in deserts is more difficult than in other regions. Calcareous root tubes are widely distributed across the deserts of the Alashan Plateau (Li et al., 2015); the presence of calcareous root tubes in the layers of paleo-dunes indicated a relatively moister climate (Yang et al., 2003; Li et al., 2015), and this study indicates that frequencies of the calcareous root tubes ^{14}C dating results on the millennial scale could indicate changes in effective moisture. Hence, more study sites and sections, especially in the hinterland of the desert, should be selected to reconstruct paleo-effective moisture changes when calcareous root tubes occurred in the layers of paleo-dunes.

However, calcareous root tubes could not indicate environments in these areas that are too humid or too arid on the millennial scale, which may lead to the areal restriction of reconstruction results compared to lake sediments and aeolian deposition. Moreover, calcareous root tubes could not indicate climate conditions during the transitional periods between extreme conditions at the centennial or decadal scale, as the accuracy of ^{14}C dating is only reliable at the millennial scale during the Holocene (Li et al., 2015). In that case, the transitional periods between two extreme climatic conditions over the shorter time scale could not be revealed by ^{14}C dating results of calcareous root tubes. Combining calcareous root tubes with multi-proxy from lake sediments or aeolian deposition may improve above-mentioned deficiencies.

5.3. Mechanisms possibly forcing changes in effective moisture

The study area is located in the marginal region of the Asian summer monsoon (Qian et al., 2007). In the Asian monsoon margin of northwestern China, millennial-scale effective moisture changes during the Holocene differed from those observed in the primary monsoon area, which experienced the most humid climate during the early Holocene (Chen et al., 2008; Li et al., 2009; Long et al., 2010; Wang et al., 2013). In this study, Holocene effective moisture changes on millennial timescales implied that the climate was arid in the early Holocene, most humid in the mid-Holocene and arid in the late Holocene. This Holocene moisture pattern is different from that in a typical Asian monsoon

area, but it is consistent with that in the Asian monsoon margin of northwestern China. The discrepancy is more likely due to the asynchronous changes in rate of evaporation and monsoon precipitation. Therefore, this difference could be caused by two factors.

The northern boundary of the Asian summer monsoon can move according to long-term climate change (Li et al., 2013a; Wang et al., 2013), and the boundary of the summer monsoon during the Holocene lay in the area between the margin of the north Qinghai–Tibet Plateau and the Tianshan Mountains in Xinjiang (Herzschuh, 2006; Chen et al., 2008). Thus, strong summer monsoons led to a relatively large increase in moisture availability in the entire desert belt of northern China (Yang et al., 2011). Moreover, low evaporation in Central and East Asia could have caused the effective moisture to increase during the mid-Holocene. Simulation results indicated that in monsoonal and arid Central Asia, low levels of lake evaporation resulted from low winter solar radiation and high summer cloud cover (Li and Morrill, 2010). Hence, higher monsoon precipitation and lower evaporation may have caused the most humid environment to occur in the mid-Holocene.

On the other hand, the greatly enhanced rate of evaporation (E) relative to the higher monsoon precipitation (P) in arid lands during the early Holocene would have reduced the effective humidity (Long et al., 2010). The Asian summer monsoon, affected by the combined effects of changes in low-latitude solar radiation and the position of the ITCZ, strengthened in the Late Glacial period and maintained its intensity until the early to mid-Holocene (Fleitmann et al., 2003; Dykoski et al., 2005; Zhang et al., 2011; Ran and Feng, 2013). However, the highest temperatures occurred in the early Holocene, as revealed by Long et al. (2010) and Thompson et al. (1997), which could have led to increased evaporation. The simulation results suggest that, in the desert margin of northern China (a part of the Asian monsoon margin), the increased evaporation in response to especially high temperatures during the early Holocene might have lowered the effective moisture enough to allow widespread dune mobility (Mason et al., 2009). Hence, increased evaporation during the early Holocene may have caused an arid environment.

6. Conclusions

The presence of calcareous root tubes indicates the occurrence of relatively humid periods in the deserts of the Alashan Plateau. We interpreted the frequency of calcareous root tubes ^{14}C dating results on the millennial scale as a proxy for effective moisture, and then we reconstructed millennial-scale changes in paleo-effective moisture during the Holocene in this area. The frequencies of 34 Holocene calcareous root tubes ^{14}C dates reveal that ~62% of the Holocene samples were dated to 7–5 cal kyr BP and ~38% of the Holocene samples were dated to 4–2 cal kyr BP. Holocene millennial-scale effective moisture changes in the deserts of the Alashan Plateau can be described as follows: an arid period during the early Holocene (before 8.0 cal kyr BP), a humid period during the mid-Holocene (8.0–5.0 cal kyr BP) and a humid to arid period during the late Holocene (after 5.0 cal kyr BP). The reconstruction results were consistent with other previous reconstruction results, which indicated that the temporal distribution of calcareous root tubes can reflect millennial-scale changes in paleo-effective moisture in this area.

However, a single sample could indicate local environmental changes that may differ from the environmental changes of the overall desert. Hence, the relatively humid environmental record obtained from the presence of calcareous root tubes is a local signal or a regional signal that should be noted. Moreover, calcareous root tubes could not indicate environments that are too humid or too arid, which may have led to the areal restriction of reconstruction results compared to lake sediments and aeolian deposition; combining calcareous root tubes with multi-proxy from lake sediments or aeolian deposition may improve this deficiency.

The Holocene moisture pattern in this area is different from that in a typical Asian monsoon area, but it is consistent with that of the Asian monsoon margin of northwestern China. The discrepancy is likely due to the asynchronous changes in the rate of evaporation and monsoon precipitation.

Acknowledgments

This work was supported by the National Natural Science Foundation of China (No. 41530745, 41301217 and 41371114) and the Fundamental Research Funds for the Central Universities (lzujbky-2015-148). The authors are grateful for the able assistance of Konglan Shao, Qing Chen and Peng Jia during field work. Dr. Paul Hesse and two anonymous reviewers are also thanked for constructive comments, which led to significant improvement of this manuscript.

References

Alonso-Zarza, A.M., 2003. Palaeoenvironmental significance of palustrine carbonates and calcretes in the geological record. Earth Sci. Rev. 60, 261–298.
An, Z., Porter, S.C., Kutzbach, J.E., Xihao, W., Suming, W., Xiaodong, L., Xiaoqiang, L., Weijian, Z., 2000. Asynchronous Holocene optimum of the East Asian monsoon. Quat. Sci. Rev. 19, 743–762.
Barta, G., 2011. Secondary carbonates in loess–paleosoil sequences: a general review. Cent. Eur. J. Geosci. 3, 129–146.
Barta, G., 2014. Paleoenvironmental reconstruction based on the morphology and distribution of secondary carbonates of the loess–paleosol sequence at Süttő, Hungary. Quat. Int. 319, 64–75.
Birkland, P., 1999. Soils and Geomorphology. Oxford University Press, New York.
Cai, Y., Zhang, H., Cheng, H., An, Z., Lawrence Edwards, R., Wang, X., Tan, L., Liang, F., Wang, J., Kelly, M., 2012. The Holocene Indian monsoon variability over the southern Tibetan Plateau and its teleconnections. Earth Planet. Sci. Lett. 335–336, 135–144.
Cerling, T.E., 1984. The stable isotopic composition of modern soil carbonate and its relationship to climate. Earth Planet. Sci. Lett. 71, 229–240.
Chen, J.S., Zhao, X., Wang, J.Y., Gu, W.Z., Sheng, X.F., Su, Z.G., 2004. Meaning of the discovery of lacustrine tufa and root-shaped nodule in Badain Jaran Desrert for the study on lake recharge. Carsologica Sin. 23, 277–282 (in Chinese with English abstract).
Chen, F., Yu, Z., Yang, M., Ito, E., Wang, S., Madsen, D.B., Huang, X., Zhao, Y., Sato, T., Birks, H. John B., Boomer, I., Chen, J., An, C., Wünnemann, B., 2008. Holocene moisture evolution in arid central Asia and its out-of-phase relationship with Asian monsoon history. Quat. Sci. Rev. 27, 351–364.
Chen, F., Li, G., Zhao, H., Jin, M., Chen, X., Fan, Y., Liu, X., Wu, D., Madsen, D., 2014. Landscape evolution of the Ulan Buh Desert in northern China during the late Quaternary. Quat. Res. 81, 476–487.
Dykoski, C., Edwards, R., Cheng, H., Yuan, D., Cai, Y., Zhang, M., Lin, Y., Qing, J., An, Z., Revenaugh, J., 2005. A high-resolution, absolute-dated Holocene and deglacial Asian monsoon record from Dongge Cave, China. Earth Planet. Sci. Lett. 233, 71–86.
Feng, Z., An, C., Wang, H., 2006. Holocene climatic and environmental changes in the arid and semi-arid areas of China: a review. The Holocene 16, 119–130.
Fleitmann, D., Burns, S.J., Mudelsee, M., Neff, U., Kramers, J., Mangini, A., Matter, A., 2003. Holocene forcing of the Indian monsoon recorded in a stalagmite from southern Oman. Science 300, 1737–1739.
Gallant, C.E., Candy, I., van den Bogaard, P., Silva, B.N., Turner, E., 2014. Stable isotopic evidence for Middle Pleistocene environmental change from a loess–paleosol sequence: Kärlich, Germany. Boreas 43, 818–833.
Gao, S., Chen, W., Jin, H., Dong, G., Li, B., Yang, G., Liu, L., Guan, Y., Sun, Z., Jin, J., 1993. Preliminary study on the Holocene desert evolution in the NW boundary of the Asia monsoon. Sci. China Ser. D 23, 202–208 (in Chinese).
Gocke, M., Kuzyakov, Y., Wiesenberg, G.L.B., 2010. Rhizoliths in loess—evidence for post-sedimentary incorporation of root-derived organic matter in terrestrial sediments as assessed from molecular proxies. Org. Geochem. 41, 1198–1206.
Gocke, M., Pustovoytov, K., Kühn, P., Wiesenberg, G.L.B., Löscher, M., Kuzyakov, Y., 2011a. Carbonate rhizoliths in loess and their implications for paleoenvironmental reconstruction revealed by isotopic composition: $\delta^{13}C$, ^{14}C. Chem. Geol. 283, 251–260.
Gocke, M., Pustovoytov, K., Kuzyakov, Y., 2011b. Carbonate recrystallization in root-free soil and rhizosphere of *Triticum aestivum* and *Lolium perenne* estimated by C-14 labeling. Biogeochemistry 103, 209–222.
Gocke, M., Gulyás, S., Hambach, U., Jovanović, M., Kovács, G., Marković, S.B., Wiesenberg, G.L.B., 2014a. Biopores and root features as new tools for improving paleoecological understanding of terrestrial sediment–paleosol sequences. Palaeogeogr. Palaeoclimatol. Palaeoecol. 394, 42–58.
Gocke, M., Hambach, U., Eckmeier, E., Schwark, L., Zöller, L., Fuchs, M., Löscher, M., Wiesenberg, G.L.B., 2014b. Introducing an improved multi-proxy approach for paleoenvironmental reconstruction of loess–paleosol archives applied on the Late Pleistocene Nussloch sequence (SW Germany). Palaeogeogr. Palaeoclimatol. Palaeoecol. 410, 300–315.
Hartmann, K., Wünnemann, B., 2009. Hydrological changes and Holocene climate variations in NW China, inferred from lake sediments of Juyanze palaeolake by factor analyses. Quat. Int. 194, 28–44.
Herzschuh, U., 2006. Palaeo-moisture evolution in monsoonal Central Asia during the last 50,000 years. Quat. Sci. Rev. 25, 163–178.

Huguet, A., Wiesenberg, G.L.B., Gocke, M., Fosse, C., Derenne, S., 2012. Branched tetraether membrane lipids associated with rhizoliths in loess: rhizomicrobial overprinting of initial biomarker record. Org. Geochem. 43, 12–19.
Jaillard, B., Guyon, A., Maurin, A., 1991. Structure and composition of calcified roots, and their identification in calcareous soils. Geoderma 50, 197–210.
Jones, B., Ng, K.C., 1988. The structure and diagenesis of rhizolites from Cayman Brac, British West Indies. J. Sediment. Petrol. 58, 457–467.
Klappa, C.F., 1980. Rhizoliths in terrestrial carbonates: classification, recognition, genesis and significance. Sedimentology 27, 613–629.
Koeniger, P., Barta, G., Thiel, C., Bajnóczi, B., Novothny, Á., Horváth, E., Techmer, A., Frechen, M., 2014. Stable isotope composition of bulk and secondary carbonates from the Quaternary loess–paleosol sequence in Süttő, Hungary. Quat. Int. 319, 38–49.
Kosir, A., 2004. Microcodium revisited: root calcification products of terrestrial plants on carbonate-rich substrates. J. Sediment. Res. 74, 845–857.
Kuzyakov, Y., Shevtzova, E., Pustovoytov, K., 2006. Carbonate re-crystallization in soil revealed by C-14 labeling: experiment, model and significance for paleo-environmental reconstructions. Geoderma 131, 45–58.
Lai, T., Wang, N., Huang, Y., Zhang, J., Zhao, L., Xu, M., 2012. Seasonal changes of lake in Tengery Desert of 2002. J. Lake Sci. 24, 957–964 (in Chinese with English abstract).
Li, Y., Morrill, C., 2010. Multiple factors causing Holocene lake-level change in monsoonal and arid central Asia as identified by model experiments. Clim. Dyn. 35, 1119–1132.
Li, Y., Wang, N., Cheng, H., Long, H., Zhao, Q., 2009. Holocene environmental change in the marginal area of the Asian monsoon: a record from Zhuye Lake, NW China. Boreas 38, 349–361.
Li, Y., Wang, N., Li, Z., Zhang, H., 2011. Holocene palynological records and their responses to the controversies of climate system in the Shiyang River drainage basin. Chin. Sci. Bull. 56, 535–546.
Li, Y., Wang, N., Li, Z., Zhang, C., Zhou, X., 2012. Reworking effects in the Holocene Zhuye Lake sediments: a case study by pollen concentrates AMS ^{14}C dating. Sci. China Earth Sci. 55, 1669–1678.
Li, Y., Wang, N., Li, Z., Zhou, X., Zhang, C., 2013a. Climatic and environmental change in Yanchi Lake, Northwest China since the Late Glacial: a comprehensive analysis of lake sediments. J. Geogr. Sci. 23, 932–946.
Li, Z., Wang, N., Li, Y., Zhang, Z., Li, M., Dong, C., Huang, R., 2013b. Runoff simulations using water and energy balance equations in the lower reaches of the Heihe River, northwest China. Environ. Earth Sci. 70, 1–12.
Li, Z., Wang, N., Cheng, H., Ning, K., Zhao, L., Li, R., 2015. Formation and environmental significance of late Quaternary calcareous root tubes in the deserts of the Alashan Plateau, northwest China. Quat. Int. 372, 167–174.
Liutkus, C.M., Wright, J.D., Ashley, G.M., Sikes, N.E., 2005. Paleoenvironmental interpretation of lake-margin deposits using δ13C and δ18O results from early Pleistocene carbonate rhizoliths, Olduvai Gorge, Tanzania. Geology 33, 377.
Long, H., Lai, Z., Wang, N., Li, Y., 2010. Holocene climate variations from Zhuyeze terminal lake records in East Asian monsoon margin in arid northern China. Quat. Res. 74, 46–56.
Long, H., Lai, Z., Fuchs, M., Zhang, J., Li, Y., 2012. Timing of Late Quaternary palaeolake evolution in Tengger Desert of northern China and its possible forcing mechanisms. Glob. Planet. Chang. 92–93, 119–129.
Ma, N., Wang, N., Zhu, J., Chen, X., Chen, H., Dong, C., 2011. Climate change around the Badain Jaran Desert in recent 50 years. J. Desert Res. 31, 1541–1547 (in Chinese with English abstract).
Ma, N., Wang, N., Zhao, L., Zhang, Z., Dong, C., Shen, S., 2014. Observation of mega-dune evaporation after various rain events in the hinterland of Badain Jaran Desert, China. Chin. Sci. Bull. 59, 162–170.
Mason, J.A., Lu, H., Zhou, Y., Miao, X., Swinehart, J.B., Liu, Z., Goble, R.J., Yi, S., 2009. Dune mobility and aridity at the desertmargin of northern China at a time of peakmonsoon strength. Geology 37, 947–950.
Mayewski, P.A., Rohling, E.E., Curt Stager, J., Karlén, W., Maasch, K.A., David Meeker, L., Meyerson, E.A., Gasse, F., van Kreveld, S., Holmgren, K., Lee-Thorp, J., Rosqvist, G., Rack, F., Staubwasser, M., Schneider, R.R., Steig, E.J., 2004. Holocene climate variability. Quat. Res. 62, 243–255.
Pustovoytov, K., Schmidt, K., Parzinger, H., 2007. Radiocarbon dating of thin pedogenic carbonate laminae from Holocene archaeological sites. The Holocene 17, 835–843.
Qian, W., Lin, X., Zhu, Y., Xu, Y., Fu, J., 2007. Climatic regime shift and decadal anomalous events in China. Clim. Chang. 84, 167–189.
Ran, M., Feng, Z., 2013. Holocene moisture variations across China and driving mechanisms: a synthesis of climatic records. Quat. Int. 313–314, 179–193.
Reimer, P.J., Bard, E., Bayliss, A., Beck, J.W., Blackwell, P.G., Bronk, R.C., Buck, C.E., Cheng, H., Edwards, R.L., Friedrich, M., Grootes, P.M., Guilderson, T.P., Haflidason, H., Hajdas, I., Hatté, C., Heaton, T.J., Hogg, A.G., Hughen, K.A., Kaiser, K.F., Kromer, B., Manning, S.W., Niu, M., Reimer, R.W., Richards, D.A., Scott, E.M., Southon, J.R., Turney, C.S.M., van der Plicht, J., 2013. IntCal13 and MARINE13 radiocarbon age calibration curves 0–50000 years cal BP. Radiocarbon 55, 1869–1887.
Thompson, L., Yao, T., Davis, M., Henderson, K., Mosley-Thompson, E., Lin, P.N., Beer, J., Synal, H.A., Cole-Dai, J., Bolzan, J., 1997. Tropical climate instability: the last glacial cycle from a Qinghai–Tibetan ice core. Science 276, 1821–1825.
Wang, T., 2003. Desert and Desertification in China. Hebei Science and Technology Press, Shijiazhuang (in Chinese).
Wang, H., Greenberg, S.E., 2007. Reconstructing the response of C_3 and C_4 plants to decadal-scale climate change during the late Pleistocene in southern Illinois using isotopic analyses of calcified rootlets. Quat. Res. 67, 136–142.
Wang, H., Ambrose, S.H., Fouke, B.W., 2004. Evidence of long-term seasonal climate forcing in rhizolith isotopes during the last glaciation. Geophys. Res. Lett. 31.
Wang, N., Li, Z., Cheng, H., Li, Y., Huang, Y., 2011. High lake levels on Alxa Plateau during the Late Quaternary. Chin. Sci. Bull. 56, 1799–1808.
Wang, N., Li, Z., Li, Y., Cheng, H., 2013. Millennial-scale environmental changes in the Asian monsoon margin during the Holocene, implicated by the lake evolution of Huahai Lake in the Hexi Corridor of northwest China. Quat. Int. 313, 100–109.
Wright, V.P., 1994. Paleosols in shallow marine carbonate sequences. Earth Sci. Rev. 35, 367–395.
Wright, V., Platt, N., Marriott, S., Beck, V., 1995. A classification of rhizogenic (root-formed) calcretes, with examples from the Upper Jurassic–Lower Cretaceous of Spain and Upper Cretaceous of southern France. Sediment. Geol. 100, 143–158.
Wu, L., 2007. Desert vegetation in Wulanbuhe and protection measures. Shaanxi For. Sci. Technol. 4, 133–137 (in Chinese with English abstract).
Wu, Y., Wang, N., Zhao, L., Zhang, Z., Chen, L., Lu, Y., Lü, X., Chang, J., 2014. Hydrochemical characteristics and recharge sources of Lake Nuoertu in the Badain Jaran Desert. Chin. Sci. Bull. 59, 886–895.
Yang, X., 2000. Landscape evolution and precipitation changes in the Badain Jaran Desert during the last 30 000 years. Chin. Sci. Bull. 45, 1042–1047.
Yang, X., Liu, T., Xiao, H., 2003. Evolution of megadunes and lakes in the Badain Jaran Desert, Inner Mongolia, China during the last 31,000 years. Quat. Int. 104, 99–112.
Yang, X., Ma, N., Dong, J., Zhu, B., Xu, B., Ma, Z., Liu, J., 2010. Recharge to the inter-dune lakes and Holocene climatic changes in the Badain Jaran Desert, western China. Quat. Res. 73, 10–19.
Yang, X., Scuderi, L., Paillou, P., Liu, Z., Li, H., Ren, X., 2011. Quaternary environmental changes in the drylands of China—a critical review. Quat. Sci. Rev. 30, 3219–3233.
Zhang, H., Ma, Y., Wünnemann, B., Pachur, H.J., 2000. A Holocene climatic record from arid northwestern China. Palaeogeogr. Palaeoclimatol. Palaeoecol. 162, 389–401.
Zhang, H., Peng, J.L., Ma, Y.Z., Chen, G.J., Feng, Z.D., Li, B., Fan, H.F., Chang, F.Q., Lei, G.L., Wünnemann, B., 2004. Late Quaternary palaeolake levels in Tengger Desert, NW China. Palaeogeogr. Palaeoclimatol. Palaeoecol. 211, 45–58.
Zhang, H., Ming, Q., Lei, G., Zhang, W., Fan, H., Chang, F., Wünnemann, B., Hartmann, K., 2006. Dilemma of dating on lacustrine deposits in an hyperarid inland basin of NW China. Radiocarbon 48, 219–226.
Zhang, J., Chen, F., Holmes, J.A., Li, H., Guo, X., Wang, J., Li, S., Lü, Y., Zhao, Y., Qiang, M., 2011. Holocene monsoon climate documented by oxygen and carbon isotopes from lake sediments and peat bogs in China: a review and synthesis. Quat. Sci. Rev. 30, 1973–1987.
Zhang, Z., Wang, N., Ma, N., Wu, Y., 2014. Lake area changes and the main causes in the hinterland of Badain Jaran Desert during 1973–2010, China. Sci. Cold Arid Reg. 6, 22–29.
Zhao, H., Li, G., Sheng, Y., Jin, M., Chen, F., 2012. Early–middle Holocene lake-desert evolution in northern Ulan Buh Desert, China. Palaeogeogr. Palaeoclimatol. Palaeoecol. 331–332, 31–38.
Zhu, Z., Wu, Z., Liu, S., 1980. An Outline of Chinese Desert. Science Press, Beijing (in Chinese).
Zhu, J., Wang, N., Chen, H., Dong, C., Zhang, H., 2010. Study on the boundary and the area of Badain Jaran Desert based on the remote sensing imagery. Prog. Geogr. 29, 1087–1094 (in Chinese with English abstract).